
ASTRA: Accurate and Scalable ANNS-based Training of Extreme Classifiers

Sonu Mehta
Microsoft Research and IIT Delhi
India
someh@microsoft.com

Jayashree Mohan
Microsoft Research
India
jamohan@microsoft.com

Nagarajan Natarajan
Microsoft Research
India
nagarajn@microsoft.com

Ramachandran Ramjee
Microsoft Research
India
ramjee@microsoft.com

Manik Varma
Microsoft Research
India
manik@microsoft.com

Abstract

“Extreme Classification” (or XC) is the task of annotating data points (queries) with relevant labels (documents), from an extremely large set of L possible labels, arising in search and recommendations. The most successful deep learning paradigm that has emerged over the last decade or so for XC is to embed the queries (and labels) using a deep encoder (e.g. DistilBERT), and use linear classifiers on top of the query embeddings. This architecture is of appeal because it enables millisecond-time inference using approximate nearest neighbor search (ANNS). The key question is how do we design training algorithms that are accurate as well as scale to $O(100M)$ labels on a limited number of GPUs.

State-of-the-art XC techniques that demonstrate high accuracies (e.g., DEXML, Renée, DEXA) on standard datasets have per-epoch training time that scales as $O(L)$ or employ expensive negative sampling strategies, which are prohibitive in XC scenarios. In this work, we develop an accurate and scalable XC algorithm ASTRA with two key observations: (a) building ANNS index on the classifier vectors and retrieving hard negatives using the classifiers aligns the negative sampling strategy to the loss function optimized; (b) keeping the ANNS indices current as the classifiers change through the epochs is prohibitively expensive while using stale negatives (refreshed periodically) results in poor accuracy; to remedy this, we propose a negative sampling strategy that uses a mixture of importance sampling and uniform sampling. By extensive evaluation on standard XC as well as proprietary datasets with 120M labels, we demonstrate that ASTRA achieves SOTA precision, while reducing training time by 4x-15x relative to the second best.

1 Introduction

We consider the *extreme classification* (XC) problem of learning to retrieve relevant labels or documents, from an extremely large corpus, for a given search phrase or query. The problem has been an active sub-field of ML research for decades now as (a) several search and recommendation problems can be formulated as a supervised learning problem with an extremely large label space; and (b) it has an enormous revenue impact on businesses, e.g., identify ads to be shown from the hundred million keywords that are bid on, when a user issues a query on the search engine.

One of the most successful paradigms for XC [9, 8, 7, 10, 2, 21] employs a deep encoder architecture for embedding the (text) queries, and, possibly also, labels; and then a linear one-vs-all style classifier

layer is applied to the embeddings to produce the final predictions for the query, i.e., the score for a (query \mathbf{x} , label ℓ) pair is the dot product of the embedding of \mathbf{x} and the classifier vector \mathbf{w}_ℓ . This paradigm is appealing because inference can be done in a few milliseconds on a CPU even with hundreds of millions of labels — by leveraging approximate nearest neighbor search (ANNS) on the trained classifier vectors to retrieve the top- k relevant labels for a given query [44]. Given a dataset with N training points and L labels, these methods crucially rely on meticulous negative mining strategies (such as clustering all the query embeddings periodically) in order to keep the per-epoch costs to $O(N * \log L)$ ($\log L$ is the number of mined negative labels per query) rather than $O(N * L)$ (L is the default number of negative labels per query). This impacts the training time significantly when the number of labels scales to tens of millions (Section 5), especially since N is typically of the same order or even larger than L .

On the other hand, recent XC algorithms like **Renée** [21] have successfully demonstrated how to *jointly train* encoder parameters and classifiers to achieve state-of-the-art accuracies on standard XC datasets. However, the training time of **Renée** scales as $O(N * L)$ as it eschews negative sampling altogether. Therefore, scaling to tens of millions of labels with **Renée** is also expensive (Section 5).

Recently, dual-encoder models like DEXML [15] have achieved state-of-the-art results on some XC datasets by using a decoupled softmax loss function. But, the lift in accuracy for DEXML comes at the cost of $O(N * L)$ training time, which prevents it from scaling to datasets beyond a few million labels.

Thus, an open question is *can we train extreme classifiers keeping the per-epoch time to $O(N * \log L)$ rather than $O(N * L)$, that would enable us scale to scenarios with hundreds of millions of labels, without compromising on the accuracy?* We propose **ASTRA**, a novel approach for jointly learning the deep encoder parameters and the extreme classifiers, formulated based on two main observations.

First, the negative mining strategy should be aligned with the training loss function; to achieve this, we have to index on the *classifier weights* (instead of label embeddings [46, 39] which is standard in literature) and *retrieve hard negatives using the indexed classifier weights*. However, this is extremely challenging to realize in practice because of the overhead of keeping the ANNS indices up-to-date with the parameter changes during training. Second, using stale indices (i.e., update indices every few epochs, and use stale hard negatives through the interim epochs) leads to poor accuracy as we show in Section 3.1. The theory of importance sampling [23] dictates that hard negatives is optimal for reducing the variance in the gradient estimates for SGD updates but empirical evidence suggests that it is no longer the case when the gradient estimates are computed using stale indices. This motivates us to design a simple, effective, *and* fast negative mining strategy — **ASTRA** uses a mixture of stale importance sampling (hard negatives) and uniform sampling (random negatives) at each iteration. We show that this mixed strategy is both efficient and achieves high accuracy. We further show that the **ASTRA** algorithm converges to a first-order stationary point at the rate of $O(1/T)$ after T iterations.

Combining random with hard negatives has been used previously to either heuristically improve performance [9] or to mitigate unstable gradients [37]. The novelty of **ASTRA** is in the insights for why a combination of random and hard negatives is needed (Section 3.1), a thorough analysis of its performance benefits, and strong empirical results on large-scale XC datasets.

To the best of our knowledge, we are the first to demonstrate that ANNS-based training of extreme classifiers is effective at the scale of hundreds of millions of labels. For instance, on a proprietary dataset with 120M labels and 370M queries, **ASTRA** achieves Precision@1 of 83.4 in 25 hours on 8 V100s. **Renée**, a state-of-the-art XC algorithm, achieves 83.8 Precision@1 but takes 375 hours or $15\times$ longer than **ASTRA** to train on the same hardware. Implementations of other state-of-the-art XC techniques [8, 10?] simply do not scale to this size. We also evaluate **ASTRA** on a number of publicly available datasets with up to 3M labels; it achieves comparable or better accuracy than state-of-the-art approaches like **Renée** or DEXML while being $4.5\times$ – $6.4\times$ faster compared to **Renée** and $14.6\times$ – $80.4\times$ faster compared to DEXML.

Our contributions are: **(1)** ANNS-based training algorithm for extreme classifiers that can scale to hundreds of millions of labels; **(2)** **ASTRA** algorithm and proof that it converges to a first-order stationary point; **(3)** **ASTRA** implementation that matches the state-of-the-art accuracy on datasets with up to 120 million labels, while reducing training times by up to $15\times$.

2 eXtreme Classification: Setup and Challenges

In the standard XC setup [18, 3, 24, 36, 19, 26], we are given a fixed set of L labels, where L can be hundreds of millions. We want to learn a prediction model f that outputs the *most relevant* subset of labels for the input query \mathbf{x} . We have access to supervised data $\{\mathbf{x}_i, \mathbf{y}_i\}_{i=1}^N$, where $\{\ell : y_{i,\ell} = 1\}$ are the subset of positive (or relevant) labels for the (text) query \mathbf{x}_i . We may also have access to textual description [33, 7, 15] or other meta-data (e.g., graphs [41, 34]) of the labels \mathbf{z}_ℓ in some scenarios.

2.1 Deep XC model design and fast inference

The most successful paradigm of XC that has emerged over the last decade or so is formulating $f_\ell(\mathbf{x}) = \langle \mathbf{w}_\ell, \mathcal{E}_\theta(\mathbf{x}) \rangle$ where $\mathcal{E}_\theta : \mathbf{x} \mapsto \mathbb{R}^d$ is a deep encoder model, such as DistilBERT [42], and $\mathbf{w}_\ell \in \mathbb{R}^d$ is the classifier vector [8, 21, 9, 33, 7] (or embedding [39, 15, 10]) for label ℓ and d is the embedding dimension. At inference time, test query \mathbf{x} is passed through the encoder $\mathcal{E}_\theta(\mathbf{x})$, and the top- k scoring labels are computed via f . In real-time applications such as search and recommendations, this design enables millisecond-time inference, as we can leverage ANNS techniques to get the top- k in time that is proportional to k (say, 10) than the extremely large L .

2.2 Challenges in scaling XC training

Dual-Encoder models: A popular XC approach is to jointly learn the embeddings of the queries and the documents (labels) using a deep encoder \mathcal{E}_θ . In each iteration, this involves computing the embeddings of both queries in the batch and all the labels. The encoder is learned using a contrastive loss that encourages the embeddings of queries to be close to their relevant documents. The learnt label embeddings are used for inference, i.e., $\mathbf{w}_\ell = \mathcal{E}_\theta(\mathbf{z}_\ell)$.

Mining useful negative labels is critical to drive the costs down to $O(N \cdot |\theta| \cdot \log L)$. The go-to strategy is choosing the “hardest negatives” [46, 15], i.e., (query, label) pair closest in the embedding space but whose ground-truth label is negative. We could leverage ANNS techniques for fast retrieval of the hard negatives but then keeping the ANNS indices current, as the embeddings change through the training epochs, adds significant overhead even when the number of labels is modest.

Classifier with Encoder models: Alternative XC approach is to not only learn the encoder (as above), but also one-vs-all style classifier vectors $\mathbf{w}_\ell \in \mathbb{R}^d$ for all the labels. This approach improves accuracy at the expense of significant increase in the number of parameters. Per-epoch time of jointly learning the encoder and the classifiers scales as $\Omega(N(Ld + |\theta|))$ and the memory requirement scales as $\Omega(Ld + |\theta|)$, where d is the embedding dimension, since all the classifiers need to be in memory.

Renée [21], state-of-the-art in this family, manages this joint training by leveraging multiple optimizations to alleviate both memory and compute bottlenecks, and using a hybrid data and model parallel training pipeline. However, the per-epoch time of Renée still scales as $O(L)$, which implies slow convergence on datasets with a few tens to hundreds of millions of labels (Section 5). Techniques like CascadeXML [27] and ELIAS [?] address scalability by learning representations at multiple resolutions or learning clustered indices of labels respectively. However, their accuracies are much worse (Section 5).

Finally, recent *modular* training methods such as NGAME [8] and DEXA [10] learn the encoder first, and then learn classifiers in the second stage using the fixed query embeddings. While this staged training helps scalability to some extent, there are compute bottlenecks such as a) computing label embeddings at every iteration, and b) an expensive clustering procedure, for negative sampling, on all the queries N which can be even larger than L (Section 5). For NGAME, balanced k -means clustering takes $O(NTk)$ time where T, k are the number of iterations and clusters. The clustering time is significantly higher than building and retrieving from ANNS indices which is typically $O(N \log L)$, as $k \gg \log L$ (Section 5.2.1).

3 ANNS-based Training of eXtreme Classifiers

We work in the XC setup introduced in Section 2.1. Our model consists of two components: the encoder network $\mathcal{E}_\theta : \mathbf{x} \mapsto \mathbb{R}^d$ and the one-vs-all classifiers \mathbf{w}_ℓ , for $\ell \in [L]$; $[L]$ is short hand for

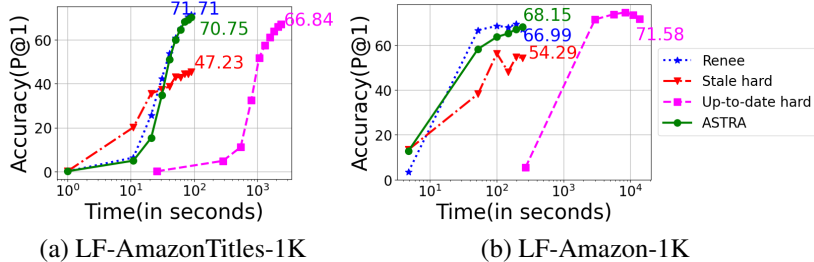


Figure 1: Training time versus Precision@1 for different negative mining strategies: *Stale hard* uses stale classifier weights, while *Up-to-date hard* builds an ANNS index on classifier weights every iteration, to sample hard negatives. *ASTRA* uses a mixture of random negatives and stale hard negatives (Section 3.1). The markers on the lines indicate epoch completion (in multiples of 5).

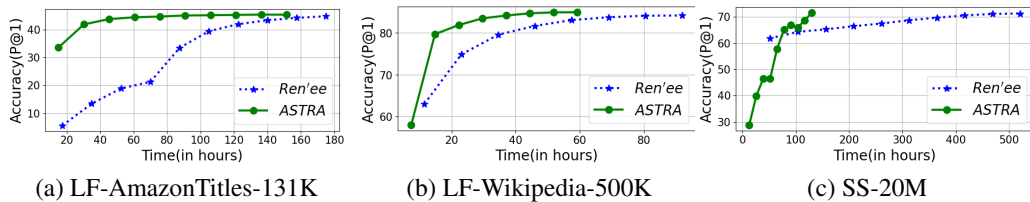


Figure 2: Training time versus P@1 for Ren'ee and ASTRA across 3 datasets. The markers on the lines indicate epoch completion (in multiples of 5).

the label set $\{1, 2, \dots, L\}$. We seek to learn f such that the top- k retrieved labels using the scores $f_\ell(\mathbf{x}) = \mathbf{w}_\ell^T \mathcal{E}_\theta(\mathbf{x})$ for input query \mathbf{x} are accurate.

Optimizing end-to-end XC loss: Ideally, we want to train all the model parameters end-to-end, which is known to achieve state-of-the-art accuracies on XC datasets [21]. That is, we want to learn the classifiers w_ℓ directly along with the encoder \mathcal{E}_θ using a suitable loss on the predicted scores $f_\ell(\mathbf{x}_i)$ and the ground-truth labels y_i . Standard loss functions used in XC training are contrastive loss such as the triplet loss [8, 10] or the binary cross entropy (BCE) loss [9, 47, 21]. In our work, we focus on the BCE loss given in equation (1) (Section 4). The key challenge is to keep the per-epoch training time to $O(N \cdot \log L)$ rather than $O(N \cdot L)$, *without* compromising on accuracy.

Compute bottleneck: Consider standard SGD updates with mini-batches to optimize the XC loss at each epoch. The per-epoch training time is dominated by backprop, i.e., computing the gradients of the loss w.r.t. encoder parameters and the L classifier weights. For triplet loss, with all the $O(L)$ negative labels per query, per-epoch time will scale as $O(N(L \cdot \log L \cdot d + |\theta|))$, as the number of positive labels per query is typically $O(\log L)$. For BCE loss, it will scale as $O(N(Ld + |\theta|))$, which is only slightly better. In either case, a major bottleneck is the dependence on L (besides N), as that trumps all other factors in the extreme settings. The reason L figures in the complexity is because the default number of negative labels per query is $O(L)$. The question then is if and how can we sample, say, $O(\log L)$ negative labels *accurately* and *efficiently* per query to remove the dependence on L .

3.1 Proposed ANNS-based negative mining strategy

Our negative mining strategy is motivated by two key observations and ideas.

Observation 1: Align the negative mining strategy with the loss. A naive solution is to directly apply ANCE-style hard negative sampling as proposed by Xiong et al. [46] (and discussed in Section 2.2) for end-to-end training of the XC model. That is, embed the labels $\mathcal{E}_\theta(\mathbf{z}_\ell)$, where \mathbf{z}_ℓ is the label meta-data, and create ANNS indices on these embeddings, and sample hard negatives for a given query from these embeddings. This is not ideal because the XC loss is computed on $\mathbf{w}_\ell^T \mathcal{E}_\theta(\mathbf{x}_i)$, but the hardest negatives are retrieved using scores based on $\mathcal{E}_\theta(\mathbf{z}_\ell)^T \mathcal{E}_\theta(\mathbf{x}_i)$ — this leads to the negative sampling strategy not being aligned with the loss. ANCE-style hard negative sampling techniques for training *encoders* [46, 25, 39] are used in conjunction with the loss function defined on the scores $\mathcal{E}_\theta(\mathbf{z}_\ell)^T \mathcal{E}_\theta(\mathbf{x}_i)$. So, the right analogue for end-to-end XC training is to create ANNS *indices on*

classifier weights rather than label embeddings and *retrieve hard negatives using the classifier weights* \mathbf{w}_ℓ . This approach not only helps aligning the indices and the negative sampling strategy to the loss, but also has the side-benefit of enabling the solution to work on datasets without label features.

Idea 1: Build ANNS-indices on classifier weights. To the best of our knowledge, there is no work in the XC community that uses indices built on classifier weights for negative sampling and achieves high accuracy at the scale of millions of labels. State-of-the-art XC techniques like NGAME [8] and DEXA [10] use the query embeddings to form mini-batches and then do in-batch negatives, while techniques like ANCE [46] and RocketQA [39] create indices on the label embeddings. While it does appear natural to use classifier weights to do negative sampling, there is a significant hurdle to realize this in practice. This leads to our second key observation.

Observation 2: Training with up-to-date negatives is prohibitively expensive while training with stale negatives results in poor accuracy. To understand how to ideally sample negatives, we can turn to the theory of importance sampling that guides optimal selection of mini-batches in SGD, i.e., how one should select mini-batches and learning rates to accelerate convergence of SGD. Proposition 3.1 of Johnson and Guestrin [23] suggests that we should select instances based on the norm of their gradients, in order to minimize the variance of the resulting gradients. We could apply the same theory to selecting negatives to estimate the loss function on a small set, instead of all negatives as in equation (1), and accelerate the convergence of SGD. For a given query \mathbf{x} , the norm of the gradient of the loss w.r.t. \mathbf{w}_ℓ is proportional to the sigmoid of the score $f_\ell(\mathbf{x}) = \langle \mathbf{w}_\ell, \mathcal{E}_\theta(\mathbf{x}) \rangle$. Thus, the ‘‘oracle’’ importance sampling strategy for the query \mathbf{x} at a given iteration t is to sample label ℓ proportional to the sigmoid of the score $\langle \mathbf{w}_\ell^{(t)}, \mathcal{E}_{\theta^{(t)}}(\mathbf{x}) \rangle$, ($^{(t)}$ denotes the latest iterate of the parameters). This requires re-creating ANNS-indices for \mathbf{w}_ℓ after every update to the parameters, which is very expensive. A practical implementation [46] is to use ‘‘stale’’ indices to do the sampling, i.e., at iteration t , we sample negative labels for query \mathbf{x} using the importance sampling distribution that is offset by some (configurable number of) iterations. To be precise, this entails using the scores $\langle \mathbf{w}_\ell^{(t')}, \mathcal{E}_{\theta^{(t')}}(\mathbf{x}) \rangle$, where $t' < t$ denotes the last iteration when the indices were refreshed. Note that we could use fresh query embeddings, i.e., $\langle \mathbf{w}_\ell^{(t')}, \mathcal{E}_{\theta^{(t)}}(\mathbf{x}) \rangle$, but in general, both can be stale, especially if we want to do this sampling asynchronously and not wait for the latest embeddings.

To understand the impact of staleness on performance, we consider small subsets of LF-AmazonTitles-131K and LF-Amazon-131K datasets by randomly sampling 1K labels and retaining all the queries that cover the 1K labels. We would like to compare the stale approach where we refresh ANNS indices every 5 epochs against the oracle sampling strategy where the ANNS indices are kept up-to-date by building fresh indices after every iteration. The oracle strategy is computationally expensive even on the 1K sampled dataset and prohibitively expensive on the full 131K dataset. Note that for these datasets, the model size is dominated by the encoder network (over 60M parameters). We initialize the encoder with pre-trained weights (trained on the full train dataset), initialize classifiers randomly, and then jointly train the encoder and classifier parameters (with tuned learning rates) using mini-batched SGD updates and BCE loss.

In Figure 1, we show the convergence of SGD for the up-to-date and stale strategies. One epoch is a pass over all queries using mini-batches of size 512 and we train for 100 epochs in total. In both the cases, instead of sampling, we retrieve 200 top-scoring negative labels (i.e., hardest negatives) from the respective distributions per query. We see that, at convergence, the accuracy of the up-to-date strategy is very close to that of the state-of-the-art solution, *Renée*, that uses all the negatives as in equation (1). But the up-to-date strategy is orders of magnitude slower than the other methods because of the sheer overhead in keeping the ANNS indices fresh with the parameter changes. On the other hand, we see that the stale strategy performs poorly. For example, on LF-AmazonTitles-1K, the converged stale solution (with a Precision@1 of 47.23) is significantly worse than the best (71.71). This observation also holds for LF-Amazon-1K as well as several XC datasets as we show in Section 5.3, and motivates us to design a better sampling strategy.

Idea 2: Use a mixture of importance sampling and uniform sampling distributions. Given a query \mathbf{x} , let $L_{\mathbf{x}}$ denote the positive label set of \mathbf{x} . We want to design a multinomial distribution over $[L] \setminus L_{\mathbf{x}}$ negative labels such that (a) it well approximates the aforementioned oracle sampling strategy, *and importantly*, (b) it allows fast sampling.

We draw inspiration from a relaxed implementation of the oracle importance sampling strategy considered by Alain et al. [1]; they propose to add a smoothing constant to the (stale) probabilities in order to be robust to variations induced by staleness in distributed SGD settings. In our experiments (Section 5.3), we find that the naïve uniform sampling of negatives is often better than stale negative

Algorithm 1: ASTRA

```
1 Init encoder  $\mathcal{E}_\theta(\mathbf{x})$ , classifiers  $\mathbf{W}$ , mini-batch size  $S$ , # hard negatives  $k_h$ , # random negatives  $k_r$ ,  
   ANNS refresh interval  $\tau_r$ , epoch to start using hard negatives  $\tau_s$ , # positives per query  $k_p$   
2 for  $epoch = 0, 1, \dots$  do  
3   Divide all data-points into random mini-batches of size  $S$   
4   for every mini-batch  $S_t$  do  
5     Embed data-points (queries) using encoder  $\mathcal{E}_{\theta^{(t)}}(\cdot)$ .  
6     if  $t < \tau_s$  then  
7       {Use random negatives to train  $\mathcal{E}_\theta(\mathbf{x})$  and  $\mathbf{W}$ }  
8       Sample  $\mathcal{N}_i$  negatives ( $=k_h+k_r$ ) uniformly at random from the feasible negative set for  
       each data point  $i \in S_t$   
9     if  $t \geq \tau_s$  and  $t \% \tau_r = 0$  then  
10      {Redo ANNS refresh at regular intervals}  
11      Use  $\mathbf{W}^{(t)}$  to build an ANNS index on.  
12      Get  $k_h$  nearest neighbours for each data-point using ANNS index, to be used until the  
       next ANNS refresh  
13     if  $t \geq \tau_s$  then  
14       {Use hard+random negatives to train  $\mathcal{E}_\theta(\mathbf{x})$  and  $\mathbf{W}$ }  
15       Get  $\mathcal{N}_i$  of negatives by sampling  $k_r$  negatives uniformly at random ( $\mathcal{R}_i$ ) and  $k_h$  hard  
       negatives ( $\mathcal{H}_i$ , most recent sample) for each data-point  $i \in S_t$   
16     Take positive labels  $\mathcal{P}_i$  ( $=k_p$ ) and sampled negative labels  $\mathcal{N}_i$  for each data point  $i \in S_t$   
17     Compute BCE loss using  $\mathcal{P}_i$  and  $\mathcal{N}_i$  as given in equation (2)  
18     Update  $\mathcal{E}_{\theta^{(t)}}(\cdot)$  using mini-batch Adam over  $S_t$  and  $\mathbf{W}^{(t)}$  using mini-batch SGD over  $S_t$ 
```

sampling strategy. So, to counter the impact of staleness, we propose a mixture distribution to sample negative labels for query \mathbf{x} at iteration t : $P^{(t)}(\mathbf{x}) = (1 - r) P_{\text{Imp}}^{(t')}(\mathbf{x}) + r P_{\text{Unif}}$, where $t' < t$ is the last ANNS index update iteration, P_{Imp} and P_{Unif} are the importance and uniform negative sampling distributions respectively, and hyperparameter $r \in [0, 1]$ governs the ratio of stale hard and uniformly random negatives. We show in Figure 1 that the proposed sampling strategy, labelled ASTRA, indeed performs nearly as good as the best. In ASTRA, we implement this strategy efficiently as follows: for a given query, we retrieve $O(\log L)$ most-likely negatives based on $P_{\text{Imp}}^{(t')}$ and c labels uniformly at random from $[L] \setminus L_{\mathbf{x}}$, where c is around 2000 for all datasets (Section 5).

3.2 ASTRA Algorithm

We present the pseudocode of our proposed method, ASTRA, in Algorithm 1. For efficiency, as discussed above, we refresh the ANNS index once every τ_r epochs (5 in our experiments) and use the same set of negatives for the interim τ_r epochs. To further reduce the overheads, we do not wait until the refresh period completely lapses to retrieve the next set of negatives. That is, if we want to use the refreshed ANNS index in epoch 10, we start saving the query embeddings in epoch 8, build and retrieve nearest neighbours from ANNS index during epoch 9, so that by the time epoch 10 starts, we have the “new” set of negatives to be used for training. All of these operations can be done asynchronously on CPUs using an ANNS module while the training epochs are underway on GPUs. Thus, ANNS-based operations do not require any additional GPU compute or memory. We discuss the cost and accuracy of ANNS index building and retrieval in Section 5.2.1.

Implementation: ASTRA implementation uses the Pytorch framework [35] and spans about 1200 lines of code. For smaller academic datasets, the implementation can be run on a single GPU, but when the number of labels are in a few millions or more, the memory requirements may be beyond the capabilities of a single GPU (e.g., 32GB V100). Therefore, following the implementation of Renée [21], ASTRA implementation has a hybrid data- and model-parallel architecture, where encoder is trained in a data-parallel fashion and the classifiers are trained in a model-parallel manner. Similar to Renée, for small datasets with labels upto $3M$, we use embedding size $d = 768$; for very large datasets, we use a bottleneck layer that reduces d to 64 and gradient accumulation to fit the required batch-sizes. We also augment the training data with label texts as training data-points in

Table 1: Results (P@ k and Training Time in hours) on the proprietary datasets with 20M and 120M labels comparing ASTRA with SOTA XC methods. The best results are in **bold**; the second best underlined. Takeaways: ASTRA matches the accuracy of SOTA Renée while being $4 \times -15 \times$ faster. NGAME is $2.3 \times$ slower, 1%-2% less accurate than ASTRA on SS-20M and does not scale to SS-120M due to the high cost of negative mining.

Methods	SS-20M (N = 146M, V = 2 GPUs)				SS-120M (N=370M, V= 8 GPUs)			
	P@1	P@5	TT (hrs)	Slowdown	P@1	P@5	TT (hrs)	Slowdown
NGAME	70.46	43.94	295.83	2.3x	Not-scalable	-	-	-
Renée	<u>71.32</u>	46.64	520.83	4x	83.78	<u>41.27</u>	375.16	15x
ASTRA	71.62	<u>46.60</u>	130.23	1x	<u>83.37</u>	41.67	25.04	1x

order to use label features for datasets wherever applicable. More details about these optimizations can be found in Appendix B.4. An ablation of ASTRA results with and without augmentation of training data with label texts is included in Table 18, Appendix C.

4 Convergence of ASTRA

Let \mathbf{W} denote the $d \times L$ matrix of classifier weights, $[L]$ denote the set of all labels, and let $\phi_{\mathbf{x}} = \mathcal{E}_{\theta}(\mathbf{x})$. For convenience, define $\mathcal{L}_+(\theta, \mathbf{W}; \mathbf{x}) := \sum_{\ell=1}^L y_{\ell} \log(1 + \exp(-\mathbf{w}_{\ell}^T \phi_{\mathbf{x}}))$, and $\mathcal{L}_-(\theta, \mathbf{W}; \mathbf{x}, \mathcal{S}) := \sum_{\ell \in \mathcal{S}} (1 - y_{\ell}) (\mathbf{w}_{\ell}^T \phi_{\mathbf{x}} + \log(1 + \exp(-\mathbf{w}_{\ell}^T \phi_{\mathbf{x}})))$. The (full) loss function that we desire to optimize is the average of losses over data-points \mathbf{x} given by:

$$\mathcal{L}(\theta, \mathbf{W}; \mathbf{x}) := \mathcal{L}_+(\theta, \mathbf{W}; \mathbf{x}) + \mathcal{L}_-(\theta, \mathbf{W}; \mathbf{x}, [L]). \quad (1)$$

Consider ASTRA at epoch t . Let $\mathcal{H}_i^{(t)}$ denote the set of hard negatives for \mathbf{x}_i sampled in Step 12, and $\mathcal{R}_i^{(t)}$ denote random negatives sampled in Step 15 of Algorithm 1. The following lemma shows two properties: (i) the BCE loss estimator in Step 17, and given below in (2) for a given \mathbf{x} , is unbiased, as are its gradients; and (ii) the gradient estimator is strongly concentrated around its expectation. For ease, we will drop the superscripts from $\mathbf{W}^{(t)}$ and $\theta^{(t)}$ when it is clear from the context.

$$\begin{aligned} \mathcal{L}_{\text{ASTRA}}^{(t)}(\theta, \mathbf{W}; \mathbf{x}) &:= \mathcal{L}_+(\theta, \mathbf{W}; \mathbf{x}) + \mathcal{L}_-(\theta, \mathbf{W}; \mathbf{x}, \mathcal{H}^{(t)}) \\ &\quad + \frac{1}{p \cdot k_r} \mathcal{L}_-(\theta, \mathbf{W}; \mathbf{x}, \mathcal{R}^{(t)}), \end{aligned} \quad (2)$$

where $p = 1/(L - k_h)$ is the probability of sampling a label uniformly at random from $[L] \setminus \mathcal{H}^{(t)}$.

Lemma 4.1. 1. Loss estimator (equation 2) is unbiased, i.e.,

$$\mathbf{E}[\mathcal{L}_{\text{ASTRA}}(\theta, \mathbf{W}; \mathbf{x})] = \mathcal{L}(\theta, \mathbf{W}; \mathbf{x}),$$

and so are the gradients computed in Step 18 of Algorithm 1.

2. For a given $\epsilon > 0$, $\delta > 0$, if $k_r = O(\log(\frac{1}{\delta}) \frac{1}{\epsilon^2})$, letting $\|\cdot\|$ be the vectorized L_2 norm, with probability at least $1 - \delta$, $\|\nabla \mathcal{L}_{\text{ASTRA}}(\theta, \mathbf{W}; \mathbf{x}) - \nabla \mathcal{L}(\theta, \mathbf{W}; \mathbf{x})\| \leq \epsilon \|\nabla \mathcal{L}(\theta, \mathbf{W}; \mathbf{x})\|$.

With these properties in place, we can now give a formal convergence result for Algorithm 1. In particular, the following theorem states that the algorithm converges to a first-order stationary point at the rate of $O(1/T)$, where the hidden (absolute) constants depend on the learning rate and the sub-optimality gap of the initial values for the model parameters. The proofs are in the Appendix A.

Theorem 4.2. Under certain smoothness assumptions (given in Appendix A.2) on the loss \mathcal{L} in (1), and under the conditions of k_r , ϵ , and δ in Lemma 4.1, for a given ϵ , if the learning rate $\eta = O(\frac{1-\epsilon}{1+\epsilon^2})$ in Step 18, Algorithm 1, after T iterations, converges to θ, \mathbf{W} s.t. $\|\nabla \mathcal{L}(\theta, \mathbf{W})\| \leq O(1/T)$.

5 Experiments

Datasets: We evaluate ASTRA on multiple short-text and long-text datasets with and without label features from the Extreme Classification Repository [4]. We also report results on proprietary datasets

Table 2: Results (P@k and Training Time in hours) on public datasets with label features comparing ASTRA with SOTA XC methods. Results for LightXML, Renée are from [21], DEXA and NGAME are from [10]; and CascadeXML and ELIAS numbers are reported from [5]. The best results are in **bold**; the second best underlined. Takeways: ASTRA performs comparable to SOTA across datasets with up-to 6.4× speed-up compared to DEXA and up-to 4.46× speed-up compared to Renée. Note that the precision values reported are of single model and not for ensembles.

Methods	LF-AmazonTitles-131K				LF-AmazonTitles-1.3M				LF-Wikipedia-500K			
	P@1	P@5	TT (hours)	Slowdown	P@1	P@5	TT (hours)	Slowdown	P@1	P@5	TT (hours)	Slowdown
DEXML	42.52	20.64	83.33	41.25x	58.40	45.46	~2000	80.45x	85.78	50.53	~592	14.67x
DEXA	45.78	21.29	13.01	6.44x	55.76	42.95	103.13	4.15x	84.92	50.51	57.51	1.42x
NGAME	44.95	21.20	12.59	6.23x	54.69	42.80	97.75	3.93x	84.01	49.97	54.88	1.36x
LightXML	35.60	17.45	71.40	35.35x			–Not-scalable–		81.59	47.64	185.56	4.60x
ELIAS	37.28	18.14	4.33	2.14x	47.48	38.6	40.00	1.61x	81.94	48.75	138.67	3.44x
CascadeXML	35.96	18.15	3.63	1.80x	47.14	37.73	70.00	2.82x	77.00	45.10	29.58	0.73x
Renée	<u>46.05</u>	22.04	2.05	1.01x	<u>56.04</u>	44.09	27.33	1.10x	<u>84.95</u>	51.68	180.00	4.46x
ASTRA	46.20	<u>21.95</u>	2.02	1.00x	55.71	<u>44.26</u>	24.86	1.00x	84.88	<u>51.30</u>	40.36	1.00x

with 20M and 120M labels. These datasets cover a variety of applications including product-to-product recommendation (Amazon-670K, Amazon-3M, LF-Amazon-131K, LF-AmazonTitles-131K, and LF-AmazonTitles-1.3M), predicting Wikipedia categories (LF-Wikipedia-500K) and matching user queries to advertiser bid phrases in sponsored search (SS-20M, SS-120M). Please refer to Appendix B.1 for more details on the datasets.

Baselines: For public datasets with label features, we compare with SOTA modular XC methods DEXA [10], NGAME [8], end-to-end XC methods LightXML [22], ELIAS [14], CascadeXML [27], Renée [21] and dual-encoder based method DEXML [15]. More comprehensive baselines are covered in Appendix C. Prior work employs ensembling to improve accuracy, which can be applied to ASTRA as well. In this paper, we report numbers based on a single model. For proprietary datasets, we compare against NGAME and Renée; available implementations of other XC aforementioned methods do not scale to $O(100M)$ labels.

Hyperparameters: We train ASTRA using Adam and SGD optimizers for the encoder and classifiers respectively. We use cosine decay with warmup learning rate schedule. On the validation set, we tune ASTRA’s hyperparameters: (i) batch-size, learning rate (lr) (ii) for the encoder, (iii) for the classifiers, (iv) dropout, (v) weight decay for classifier, (vi) number of random negatives (k_r), (vii) number of hard negatives (k_h), (viii) starting epoch for hard negative sampling (τ_s), (ix) refresh frequency for ANNS index (τ_r). ASTRA is fairly robust to the choice of hyperparameters (specific to our algorithm) τ_s , τ_r , k_r and k_h as shown in Tables 6, 7 and 8 (discussed in Section 5.2.1). Appendix B.2 has details on tuning and the chosen hyperparameter values. The hyperparameters for baseline methods were set as per the respective papers.

Evaluation Metrics: Models are evaluated using Precision@k (P@k, $k \in 1, 5$) and training time (All models are run on V100 GPUs). Results on other metrics, such as P@3, propensity-scored [20, 38, 43] variants of Precision@k (PSP@k, $k \in 1, 3, 5$), nDCG@k (N@k) and PSN@k [20, 38, 43] are reported in Appendix C. Please refer to [4] for definitions of all these metrics.

5.1 Accuracy and Efficiency of ASTRA on the largest datasets

We evaluate the performance of ASTRA on the two largest (proprietary) datasets with 20M and 120M labels. As mentioned early in this section, the available XC implementations that scale to these sizes are Renée and NGAME. Table 1 shows that **ASTRA** matches the *state-of-the-art* (Precision@k, $k \in 1, 5$) **with 4× and 15× speed-up** in the training time for SS-20M (where all the methods are run on 2 GPUs) and SS-120M (where all the methods are run on 8 GPUs) datasets respectively.

5.2 Accuracy, Efficiency, and Memory Footprint Analysis of ASTRA on public datasets

(a) Accuracy: Table 2 compares ASTRA with baseline and SOTA XC methods on three public datasets with label features. We observe that ASTRA matches the SOTA Precision@k, $k \in \{1, 5\}$ on all the datasets except P@1 for LF-AmazonTitles-1.3M. Further, ASTRA achieves up to 80× speed-up in training time compared to DEXML and up to 4.5× speed-up compared to Renée on 1 V100 GPU. Note that the precision values reported are of single model and not for ensembles (Appendix C has ensemble results). We observe similar trends on datasets without label features presented in Appendix C due to space constraints.

Table 3: Break-up of iteration time (in milliseconds) of ASTRA and Renée for three datasets. *The optimized version of Renée does not calculate loss, hence marked as N/A.

Dataset	LFAT-131K		LFAT-1.3M		SS-20M	
Method	Renée	ASTRA	Renée	ASTRA	Renée	ASTRA
1.DataPrep	0.1	0.2	0.1	0.2	0.1	0.2
2.CopyToGPU	0.3	0.3	0.3	0.3	0.3	0.3
3.EncFwdPass	14.3	14.2	14.4	14.4	14.3	14.5
4.ClffwdPass	0.6	1.3	5.4	1.4	76.8	1.6
5.LossCalc	N/A*	0.3	N/A	0.3	N/A	0.3
6.BwdPass	20.4	21.9	39.6	31.6	183.3	32.2
7.Sum	35.4	38.2	98.3	48.1	274.8	49.1

(b) Efficiency: As mentioned in Section 3.1, the key advantage in training time comes from negative mining which reduces the per-epoch complexity to $O(N(\log L \cdot d + |\theta|))$ from $O(N(Ld + |\theta|))$ of Renée. The per-epoch computation of ASTRA is dominated by the 6 steps shown in Table 3. First, note that $O(\log L)$ vs $O(L)$ scaling is applicable only to the classifier forward (and the overall backward) pass steps, i.e., rows 4 and 6, and the loss calculation (row 5). Clearly, classifier forward and backward pass are the dominating values for large values of L as seen from Table 3; and we see that Renée’s compute scales linearly in L , as we go from left to right in the Table. On the other hand, for ASTRA, the classifier forward pass remains more or less the same (around 1.5 ms), with very small variation across L . $O(\log L)$ scaling is not apparent here because the compute in steps 4 and 6 is dominated not by the $\log L$ sampled hard negatives per query, but by the constant but relatively larger number of random negatives per query. Because we use a constant number of random negatives per query (around 2000, $\gg O(\log L)$ and independent of L , as shown in Table 11 of Appendix B.2), the compute remains almost constant for ASTRA in Table 3, from left to right. This represents the key efficiency gain of ASTRA compared to Renée, while also being competitive or even outperforming Renée in the extreme regime, as seen from Tables 1 and 2.

Practical applications have a training budget. Figure 2 shows that ASTRA converges much faster compared to Renée consistently across datasets. For smaller L values, the overall speed-up is not significant for aforementioned reasons.

(c) Memory Footprint: Table 4 compares CPU and GPU memory usage of ASTRA with Renée. Overall, negative sampling in ASTRA leads to upto $668\times$ reduction in GPU memory compared to Renée. For the classifier forward pass, Renée uses $O(S \cdot L)$ GPU memory to save the output of matrix multiplications where S is mini batch-size. ASTRA uses $O(S \cdot \log L)$ memory as the matrix multiplication is done with positives and selected negatives.

5.2.1 ANNS - Overheads, Accuracy and Efficiency

ANNS index is built on CPU and the retrieved negatives are stored as memmap files, after which the ANNS index is discarded. Memmap files are loaded into RAM during training. Table 4 (‘CPU’ column) shows that the additional CPU memory usage because of these memmap files is very low. As described in Section 3.2, ASTRA does not use any additional GPU memory to save or retrieve from ANNS indices.

a) **Accuracy of ANNS:** To investigate the accuracy of sampled hard negatives, we compare two ANNS indices, DiskANN [45] and Faiss [11], in ASTRA. The recall values of both these techniques are similar (92.5% – 95% across datasets), and in particular recall $> 90\%$ for both the techniques across datasets (recall is defined as the fraction of the true nearest neighbors retrieved by an ANNS algorithm). To further investigate the impact of ANNS choice in ASTRA, we trained ASTRA using *exact search* (recall is 100%, by definition) for small datasets (LF-AmazonTitles-131K, LF-Amazon-131K) instead of ANNS, keeping all other hyperparameters the same. Even in this exact setting, we do not observe any significant gains in terms of our final evaluation metrics on these datasets.

b) **Efficiency of ANNS:** Building ANNS index (e.g., DiskANN) typically costs $O(L \cdot \log L)$ time. The time complexity to retrieve k nearest neighbours for N queries from the ANNS index is $O(N \cdot k \cdot \log L)$. So, the total time to build and retrieve from ANNS index is $O(N \cdot \log L)$, since

Table 4: Memory usage (in MB) of ASTRA and Renée on public datasets. Reduction in GPU memory usage is in parantheses.

Dataset	GPU		CPU	
	Renée	ASTRA	Renée	ASTRA
LF-Amazonitles-131K	128.00	2.06 (62.2x)	0	1.35
LF-Amazon-131K	128.00	1.91 (67.1x)	0	0.68
Amazon-670K	327.19	3.57 (91.6x)	0	1.34
LF-AmazonTitles-1.3M	2549.35	3.81 (668.7x)	0	1.49
Amazon-3M	1373.18	3.91 (351.5x)	0	1.62

Table 5: Ablative study (Section 3.1) of negative sampling strategies in ASTRA: In all the rows, # negative labels per query is fixed (to 2K). Hard negatives obtained using label embeddings are “ \mathcal{E}_θ -hard”; those obtained using classifiers are “ w -hard”. *All the hard negatives are stale (refreshed every 5 epochs)*. The best results are in **bold**; the second best underlined.

Methods	LF-AmazonTitles-131K		LF-Amazon-131K		LF-Wikipedia-500K	
	P@1	P@5	P@1	P@5	P@1	P@5
random	44.57	<u>21.83</u>	45.62	22.9	72.49	44.58
\mathcal{E}_θ hard	41.98	19.07	15.39	8.65	57.37	28.87
curriculum Learning (\mathcal{E}_θ hard)	<u>45.84</u>	21.75	43.81	21.25	74.35	46.24
random + \mathcal{E}_θ hard	45.55	21.55	45.79	22.15	81.40	47.60
w hard	41.74	20.79	17.86	8.87	52.84	22.92
curriculum Learning (w hard)	<u>45.83</u>	21.58	47.33	22.47	<u>84.56</u>	51.72
random + w hard (ASTRA)	46.20	21.95	<u>47.13</u>	<u>22.35</u>	84.88	<u>51.30</u>

$N > L$ for most XC datasets (shown in Table 5 in Appendix B.1). For ASTRA, the per-epoch training time scales as $O(N(\log L \cdot d + |\theta|))$; so, building and retrieving from ANNS index can be done within an epoch’s time, and we observe this in practice across datasets as well.

5.3 Ablative study on the negative sampling strategy of ASTRA

We perform ablative study on the two design choices of ASTRA presented in Section 3.1. **(1) building the ANNS index on the classifier weights:** A natural question is what if we built indices and sampled negatives using *the label embeddings* instead, keeping all other choices in Algorithm 1 fixed. We observe from the Table 5 that the proposed strategy of using classifier weights outperforms using label embeddings (in rows 2 and 3, denoted by \mathcal{E}_θ -hard) across three datasets. **(2) the proposed mixture of stale hard and uniform distribution for sampling negatives:** We make two observations in this regard. First, we see that the proposed mixture distribution (last row) significantly outperforms using stale hard negatives (denoted by w -hard). This reinforces our observations in Section 3.1 and Figure 1. Second, the mixture distribution helps even when we use label embeddings for sampling, comparing rows 2 and 3. Finally, we compare curriculum learning, i.e., we start with random negatives and gradually increase the ratio of stale hard and random negatives through the epochs. We observe that the curriculum learning using classifier weights outperforms using label embeddings.

6 Related Work

We highlight XC techniques, especially negative mining, not addressed thus far.

In-batch negatives: In this strategy, for a given query in a mini-batch, the positive labels of other queries in the mini-batch are treated as its negatives. This is one of the most popular strategies for representation learning in the unsupervised [12, 31, 6, 16] as well as in the (partially) supervised learning settings [25, 28]. Dahiya et al. [7] use a variant of this approach, by forming mini-batches on *labels* and mining the hardest few queries within the mini-batch instead.

(Semi-)Global retrieval: Here, the negatives are retrieved globally from the full label set [13, 40, 25, 30, 46]. Xiong et al. [46] propose ANCE method, that retrieves hard negatives via a global index of labels that is asynchronously updated (every few iterations). However, as we show in Section 5.3, this strategy compromises on the accuracy. In the *stochastic negative mining* strategy proposed by

Table 6: Performance of ASTRA with different values of k_h, k_r (sampled hard and random negatives) on two datasets.

k_h, k_r	LF-AmazonTitles-131K		LF-Wikipedia-500K	
	P@1	P@5	P@1	P@5
50:400	46.20	21.95	84.88	51.30
50:300	46.25	21.92	84.14	50.77
50:200	46.23	21.89	84.10	50.21
50:100	46.17	21.79	83.07	49.67
30:400	46.15	21.91	84.09	50.70
30:100	46.12	21.75	84.02	50.67
20:400	46.10	21.92	84.03	50.63
20:300	46.12	21.89	84.01	50.64

Table 7: Performance of ASTRA with varying τ_s (the starting epoch for hard negative sampling) on two datasets.

τ_s	LF-Amazon-131K		LF-AmazonTitles-1.3M	
	P@1	P@5	P@1	P@5
5	47.13	22.35	55.71	44.26
10	46.29	21.96	52.17	41.40
20	46.24	21.97	51.76	41.28

Reddi et al. [40], a batch B of negatives is first sampled uniformly at random globally, and then the top- k hardest negatives are obtained from within the batch, where typically $k \ll B$. To strike a fine balance between memory- and compute-efficiency, and accuracy, semi-global retrieval strategies have been proposed [39, 17, 8]. Qu et al. [39] propose a “cross-batch” mining strategy for data-parallel training on multiple GPUs, where they include the negatives from the other mini-batches (on different GPUs). Further, to mitigate the risk of including false negatives, they train a cross-encoder to filter out potential false negatives, and retain only the high-scoring (hard) negatives.

Streaming/caching strategies: He et al. [16] maintain a streaming label cache (negatives) for updating the encoder parameters. Lindgren et al. [32] use the Gumbel-Max technique to sample negatives from the softmax distribution. For efficiency, they first sample a large multi-set of items (“negative cache”), and update the oldest few embeddings in the cache at every iteration.

7 Conclusions, Limitations and Future Work

We show that it is indeed viable to do ANNS-based training of extreme classifiers in a scalable fashion, and achieve SOTA accuracies. The prevailing wisdom in the information retrieval community of using hard (but stale) negatives to train encoders does not extend to XC training as we demonstrate in this work. We motivate our approach using empirical observations, guided by theoretical insights from the optimization community. We show that ASTRA scales to 100M labels with an order of magnitude less training time than the previous SOTA, while matching the accuracies. One limitation of our approach is that scaling to $L = O(1B)$ brings a new set of challenges because the ANNS indexing will start to become the bottleneck. Solving this challenge might require a new algorithm for ANNS or perhaps a completely new approach for XC. We believe similar ANNS-based training strategies can be more broadly applied, for instance, to scaling NGAME [8] and DEXA [10], which opens up exciting new frontiers for further research in XC.

Table 8: Performance of ASTRA with different values of τ_r (refresh frequency for ANNS index) on two datasets.

τ_r	LF-Amazon-131K		LF-AmazonTitles-1.3M	
	P@1	P@5	P@1	P@5
5	47.13	22.35	55.71	44.26
10	46.28	21.95	50.43	40.04
20	46.02	21.84	47.82	29.06

References

- [1] Guillaume Alain, Alex Lamb, Chinnadhurai Sankar, Aaron Courville, and Yoshua Bengio. 2015. Variance reduction in SGD by distributed importance sampling. *arXiv preprint arXiv:1511.06481* (2015).
- [2] Anonymous. 2019. Source code and datasets for DeepXML. In *Anonymous*.
- [3] R. Babbar and B. Schölkopf. 2017. DiSMEC: Distributed Sparse Machines for Extreme Multi-label Classification. In *WSDM*.
- [4] K. Bhatia, K. Dahiya, H. Jain, P. Kar, A. Mittal, Y. Prabhu, and M. Varma. 2016. The Extreme Classification Repository: Multi-label Datasets & Code. <http://manikvarma.org/downloads/XC/XMLRepository.html>
- [5] Anirudh Buvanesh, Rahul Chand, Jatin Prakash, Bhawna Paliwal, Mudrit Dhawan, Neelabh Madan, Deepesh Hada, Vidit Jain, SONU MEHTA, Yashoteja Prabhu, Manish Gupta, Ramachandran Ramjee, and Manik Varma. 2024. Enhancing Tail Performance in Extreme Classifiers by Label Variance Reduction. In *The Twelfth International Conference on Learning Representations*. <https://openreview.net/forum?id=6AR1Sgun7J>
- [6] T. Chen, S. Kornblith, M. Norouzi, and G. Hinton. 2020. A simple framework for contrastive learning of visual representations. In *ICML*.
- [7] K. Dahiya, A. Agarwal, D. Saini, K. Gururaj, J. Jiao, A. Singh, S. Agarwal, P. Kar, and M. Varma. 2021. SiameseXML: Siamese Networks meet Extreme Classifiers with 100M Labels. In *ICML*.
- [8] K. Dahiya, N. Gupta, D. Saini, A. Soni, Y. Wang, K. Dave, J. Jiao, K. Gururaj, P. Dey, A. Singh, D. Hada, V. Jain, B. Paliwal, A. Mittal, S. Mehta, R. Ramjee, S. Agarwal, P. Kar, and M. Varma. 2023. NGAME: Negative mining-aware mini-batching for extreme classification. In *WSDM*.
- [9] K. Dahiya, D. Saini, A. Mittal, A. Shaw, K. Dave, A. Soni, H. Jain, S. Agarwal, and M. Varma. 2021. DeepXML: A Deep Extreme Multi-Label Learning Framework Applied to Short Text Documents. In *WSDM*.
- [10] Kunal Dahiya, Sachin Yadav, Sushant Sondhi, Deepak Saini, Sonu Mehta, Jian Jiao, Sumeet Agarwal, Purushottam Kar, and Manik Varma. 2023. Deep Encoders with Auxiliary Parameters for Extreme Classification. In *Proceedings of the 29th ACM SIGKDD Conference on Knowledge Discovery and Data Mining (<conf-loc>, <city>Long Beach</city>, <state>CA</state>, <country>USA</country>, </conf-loc>)* (KDD '23). New York, NY, USA, 358–367.
- [11] Matthijs Douze, Alexandr Guzhva, Chengqi Deng, Jeff Johnson, Gergely Szilvasy, Pierre-Emmanuel Mazaré, Maria Lomeli, Lucas Hosseini, and Hervé Jégou. 2024. The Faiss library. (2024). arXiv:2401.08281 [cs.LG]
- [12] F. Faghri, D.-J. Fleet, J.-R. Kiros, and S. Fidler. 2018. VSE++: Improving Visual-Semantic Embeddings with Hard Negatives. In *BMVC*.
- [13] C. Guo, A. Mousavi, X. Wu, D.-N. Holtmann-Rice, S. Kale, S. Reddi, and S. Kumar. 2019. Breaking the Glass Ceiling for Embedding-Based Classifiers for Large Output Spaces. In *NeurIPS*.
- [14] Nilesh Gupta, Patrick H. Chen, Hsiang-Fu Yu, Cho-Jui Hsieh, and Inderjit S. Dhillon. 2022. ELIAS: End-to-End Learning to Index and Search in Large Output Spaces. In *Advances in Neural Information Processing Systems 35: Annual Conference on Neural Information Processing Systems 2022, NeurIPS 2022, New Orleans, LA, USA, November 28 - December 9, 2022*, Sanmi Koyejo, S. Mohamed, A. Agarwal, Danielle Belgrave, K. Cho, and A. Oh (Eds.). http://papers.nips.cc/paper_files/paper/2022/hash/7d4f98f916494121aca3da02e36a4d18-Abstract-Conference.html
- [15] Nilesh Gupta, Devvrit, Ankit Singh Rawat, Srinadh Bhojanapalli, Prateek Jain, and Inderjit S. Dhillon. 2024. Dual-Encoders for Extreme Multi-label Classification. In *The Twelfth International Conference on Learning Representations, ICLR 2024, Vienna, Austria, May 7-11, 2024*. OpenReview.net. <https://openreview.net/forum?id=dNe1T0Ahby>

- [16] K. He, Haoqi Fan, Yuxin W., S. Xie, and R. Girshick. 2020. Momentum contrast for unsupervised visual representation learning. In *CVPR*.
- [17] S. Hofstätter, S.-C. Lin, J.-H. Yang, J. Lin, and A. Hanbury. 2021. Efficiently Teaching an Effective Dense Retriever with Balanced Topic Aware Sampling. In *SIGIR*.
- [18] P. S. Huang, X. He, J. Gao, L. Deng, A. Acero, and L. Heck. 2013. Learning Deep Structured Semantic Models for Web Search using Clickthrough Data. In *CIKM*.
- [19] H. Jain, V. Balasubramanian, B. Chunduri, and M. Varma. 2019. Slice: Scalable Linear Extreme Classifiers trained on 100 Million Labels for Related Searches. In *WSDM*.
- [20] H. Jain, Y. Prabhu, and M. Varma. 2016. Extreme Multi-label Loss Functions for Recommendation, Tagging, Ranking and Other Missing Label Applications. In *KDD*.
- [21] Vidit Jain, Jatin Prakash, Deepak Saini, Jian Jiao, Ramachandran Ramjee, and Manik Varma. 2023. Renee: End-to-end training of extreme classification models. *Proceedings of Machine Learning and Systems (2023)*.
- [22] T. Jiang, D. Wang, L. Sun, H. Yang, Z. Zhao, and F. Zhuang. 2021. LightXML: Transformer with Dynamic Negative Sampling for High-Performance Extreme Multi-label Text Classification. In *AAAI*.
- [23] Tyler B Johnson and Carlos Guestrin. 2018. Training deep models faster with robust, approximate importance sampling. *Advances in Neural Information Processing Systems* 31 (2018).
- [24] A. Joulin, E. Grave, P. Bojanowski, and T. Mikolov. 2017. Bag of Tricks for Efficient Text Classification. In *EACL*.
- [25] V. Karpukhin, B. Oguz, S. Min, P. Lewis, L. Wu, S. Edunov, D. Chen, and W.-T. Yih. 2020. Dense Passage Retrieval for Open-Domain Question Answering. In *EMNLP*.
- [26] S. Khandagale, H. Xiao, and R. Babbar. 2020. Bonsai: diverse and shallow trees for extreme multi-label classification. *ML (2020)*.
- [27] S. Kharbanda, A. Banerjee, E. Schultheis, and R. Babbar. 2022. CascadeXML: Rethinking Transformers for End-to-end Multi-resolution Training in Extreme Multi-label Classification. In *NeurIPS*.
- [28] Prannay Khosla, Piotr Teterwak, Chen Wang, Aaron Sarna, Yonglong Tian, Phillip Isola, Aaron Maschinot, Ce Liu, and Dilip Krishnan. 2020. Supervised contrastive learning. *Advances in neural information processing systems* 33 (2020), 18661–18673.
- [29] Jonas Moritz Kohler and Aurelien Lucchi. 2017. Sub-sampled cubic regularization for non-convex optimization. In *International Conference on Machine Learning*. PMLR, 1895–1904.
- [30] B. G. V. Kumar, B. Harwood, G. Carneiro, I. D. Ian D. Reid, and T. Drummond. 2017. Smart Mining for Deep Metric Learning. In *ICCV*.
- [31] K. Lee, M.-W. Chang, and K. Toutanova. 2019. Latent retrieval for weakly supervised open domain question answering. In *ACL*.
- [32] Erik Lindgren, Sashank Reddi, Ruiqi Guo, and Sanjiv Kumar. 2021. Efficient training of retrieval models using negative cache. *Advances in Neural Information Processing Systems* 34 (2021), 4134–4146.
- [33] A. Mittal, K. Dahiya, S. Agrawal, D. Saini, S. Agarwal, P. Kar, and M. Varma. 2021. DECAF: Deep Extreme Classification with Label Features. In *WSDM*.
- [34] A. Mittal, N. Sachdeva, S. Agrawal, S. Agarwal, P. Kar, and M. Varma. 2021. ECLARE: Extreme Classification with Label Graph Correlations. In *WWW*.

- [35] Adam Paszke, Sam Gross, Francisco Massa, Adam Lerer, James Bradbury, Gregory Chanan, Trevor Killeen, Zeming Lin, Natalia Gimelshein, Luca Antiga, Alban Desmaison, Andreas Köpf, Edward Yang, Zach DeVito, Martin Raison, Alykhan Tejani, Sasank Chilamkurthy, Benoit Steiner, Lu Fang, Junjie Bai, and Soumith Chintala. 2019. PyTorch: An Imperative Style, High-Performance Deep Learning Library. arXiv:1912.01703 [cs.LG]
- [36] Y. Prabhu, A. Kag, S. Harsola, R. Agrawal, and M. Varma. 2018. Parabel: Partitioned label trees for extreme classification with application to dynamic search advertising. In *WWW*.
- [37] Mohammadreza Qaraei and Rohit Babbar. 2023. Meta-classifier free negative sampling for extreme multilabel classification. *Mach. Learn.* 113, 2 (nov 2023), 675–697. <https://doi.org/10.1007/s10994-023-06468-w>
- [38] M. Qaraei, E. Schultheis, P. Gupta, and R. Babbar. 2021. Convex Surrogates for Unbiased Loss Functions in Extreme Classification With Missing Labels. In *The WebConf*.
- [39] Yingqi Qu, Yuchen Ding, Jing Liu, Kai Liu, Ruiyang Ren, Wayne Xin Zhao, Daxiang Dong, Hua Wu, and Haifeng Wang. 2021. RocketQA: An Optimized Training Approach to Dense Passage Retrieval for Open-Domain Question Answering. In *Proceedings of the 2021 Conference of the North American Chapter of the Association for Computational Linguistics: Human Language Technologies*. 5835–5847.
- [40] S. J. Reddi, S. Kale, F.X. Yu, D. N. H. Rice, J. Chen, and S. Kumar. 2019. Stochastic Negative Mining for Learning with Large Output Spaces. In *AISTATS*.
- [41] D. Saini, A.K. Jain, K. Dave, J. Jiao, A. Singh, R. Zhang, and M. Varma. 2021. GalaXC: Graph Neural Networks with Labelwise Attention for Extreme Classification. In *WWW*.
- [42] V. Sanh, L. Debut, J. Chaumond, and T. Wolf. 2019. DistilBERT, a distilled version of BERT: smaller, faster, cheaper and lighter. *ArXiv* (2019).
- [43] E. Schultheis, M. Wydmuch, R. Babbar, and K. Dembczynski. 2022. On Missing Labels, Long-Tails and Propensities in Extreme Multi-Label Classification. In *KDD*.
- [44] Harsha Vardhan Simhadri, Ravishankar Krishnaswamy, Gopal Srinivasa, Suhas Jayaram Subramanya, Andrija Antonijevic, Dax Pryce, David Kaczynski, Shane Williams, Siddarth Golapudi, Varun Sivashankar, Neel Karia, Aditi Singh, Shikhar Jaiswal, Neelam Mahapatro, Philip Adams, Bryan Tower, and Yash Patel. 2023. DiskANN: Graph-structured Indices for Scalable, Fast, Fresh and Filtered Approximate Nearest Neighbor Search. <https://github.com/Microsoft/DiskANN>
- [45] S. J. Subramanya, Devvrit, R. Kadekodi, R. Krishnaswamy, and H. Simhadri. 2019. DiskANN: Fast Accurate Billion-point Nearest Neighbor Search on a Single Node. In *NeurIPS*.
- [46] Lee Xiong, Chenyan Xiong, Ye Li, Kwok-Fung Tang, Jialin Liu, Paul N Bennett, Junaid Ahmed, and Arnold Overwijk. 2020. Approximate Nearest Neighbor Negative Contrastive Learning for Dense Text Retrieval. In *International Conference on Learning Representations*.
- [47] Xiaohua Zhai, Basil Mustafa, Alexander Kolesnikov, and Lucas Beyer. 2023. Sigmoid Loss for Language Image Pre-Training. *arXiv e-prints* (2023), arXiv–2303.

A Proofs

A.1 Proof of Lemma 4.1

(1) The first part of the Lemma is easy to show. Note that the expectation is with respect to the randomness in the sampling of negative labels with uniform probability $p = 1/(L - k_h)$ from the set $[L] \setminus \mathcal{H}$. Comparing the full loss (1) and the estimator in (2), it suffices to show that $\mathcal{L}_-(\boldsymbol{\theta}, \mathbf{W}; \mathbf{x}, \mathcal{H}) + \frac{1}{p \cdot k_r} \mathbf{E}[\mathcal{L}_-(\boldsymbol{\theta}, \mathbf{W}; \mathcal{R})] = \mathcal{L}_-(\boldsymbol{\theta}, \mathbf{W}; \mathbf{x}; [L])$. This is true because $\mathbf{E}[\mathcal{L}_-(\boldsymbol{\theta}, \mathbf{W}; \mathbf{x}, \mathcal{R})] = \frac{k_r}{(L - k_h)} \sum_{\ell \in [L] \setminus \mathcal{H}} \mathcal{L}_-(\boldsymbol{\theta}, \mathbf{W}; \mathbf{x}, \{\ell\}) = \frac{k_r}{(L - k_h)} \mathcal{L}_-(\boldsymbol{\theta}, \mathbf{W}; \mathbf{x}, [L] \setminus \mathcal{H}) = p \cdot k_r \mathcal{L}_-(\boldsymbol{\theta}, \mathbf{W}; \mathbf{x}, [L] \setminus \mathcal{H})$. The same argument holds for gradients as well.

(2) Now consider the second part of the lemma, which is about concentration of gradients around its expectation. For ease of presentation, we will work with mini-batch of size 1, i.e., the query data-point \mathbf{x} , and we will elide the arguments from the loss functions using “.” when it’s clear from the context.

(2.1) First, let us consider the gradient of $\mathcal{L}_{\text{ASTRA}}$ with respect to $\boldsymbol{\theta}$. Our goal is to bound the likelihood of the bad event that $\|\nabla_{\boldsymbol{\theta}} \mathcal{L}_{\text{ASTRA}}(\cdot; \mathbf{x}) - \nabla_{\boldsymbol{\theta}} \mathcal{L}(\cdot; \mathbf{x})\| \geq \epsilon \|\nabla_{\boldsymbol{\theta}} \mathcal{L}(\cdot; \mathbf{x})\|$, for a given $\epsilon > 0$.

Firstly, recall from the first part of the proof that the losses $\mathcal{L}_{\text{ASTRA}}$ and \mathcal{L} , and therefore gradients, differ exactly in the part of the loss function where we do random negative sampling, and the remainder is identical across the two loss functions. Thus,

$$\|\nabla_{\boldsymbol{\theta}} \mathcal{L}_{\text{ASTRA}}(\cdot; \mathbf{x}) - \nabla_{\boldsymbol{\theta}} \mathcal{L}(\cdot; \mathbf{x})\| = \left\| \frac{1}{p \cdot k_r} \nabla_{\boldsymbol{\theta}} \mathcal{L}_-(\cdot; \mathbf{x}, \mathcal{R}) - \nabla_{\boldsymbol{\theta}} \mathcal{L}_-(\cdot; \mathbf{x}, [L] \setminus \mathcal{H}) \right\|. \quad (3)$$

Now let

$$\hat{Z}_{\ell} = \frac{1}{p} \nabla_{\boldsymbol{\theta}} \mathcal{L}_-(\cdot; \mathbf{x}, \{\ell\}),$$

and let

$$Z := \nabla_{\boldsymbol{\theta}} \mathcal{L}_-(\cdot; \mathbf{x}, [L] \setminus \mathcal{H}).$$

Now, we can rewrite RHS of (3) as:

$$\|\nabla_{\boldsymbol{\theta}} \mathcal{L}_{\text{ASTRA}}(\cdot; \mathbf{x}) - \nabla_{\boldsymbol{\theta}} \mathcal{L}(\cdot; \mathbf{x})\| = \left\| \frac{1}{k_r} \sum_{\ell \in \mathcal{R}} \hat{Z}_{\ell} - Z \right\|. \quad (4)$$

Note that since $\mathbb{E}[\hat{Z}_{\ell}] = Z$, we have average of independent, vector-valued, zero-mean random variables in (4). Further, we can bound $\mathbb{E}[\|\hat{Z}_{\ell}\|] = \frac{1}{p} E \left[\left\| \frac{-1}{1 + \exp(-\mathbf{w}_{\ell}^T \phi(\mathbf{x}))} \mathbf{w}_{\ell} \nabla_{\boldsymbol{\theta}} \phi(\mathbf{x}) \right\| \right] \leq \frac{1}{p} \|\mathbf{w}_{\ell}\| \|\nabla_{\boldsymbol{\theta}} \phi(\mathbf{x})\| \leq \mu = \mathcal{O}(L)$, where the hidden constants depend on the Lipschitz-constant of the encoder function $\mathcal{E}_{\boldsymbol{\theta}}(\mathbf{x})$, and the (bounded) norm of the classifiers. Similarly we can bound the second moment as $\mathbb{E}[\|\hat{Z}_{\ell}\|^2] \leq \sigma^2 = \mathcal{O}(L^2)$.

Now we can appeal to the vector version of Bernstein’s inequality as given in Lemma 18 of Kohler and Lucchi [29], Appendix A, as all the necessary quantities satisfy the pre-requisites of the Lemma. We have, for $0 < \epsilon' < \sigma^2/\mu$,

$$P \left(\left\| \frac{1}{k_r} \sum_{\ell \in \mathcal{R}} \hat{Z}_{\ell} - Z \right\| \geq \epsilon' \right) \leq 2 \exp \left(-k_r \cdot \frac{\epsilon'^2}{8\sigma^2} \right).$$

Now, let’s substitute $\epsilon' = \epsilon \|\nabla_{\boldsymbol{\theta}} \mathcal{L}(\cdot; \mathbf{x})\|$, which is the bound we seek. This is permissible as $\|\nabla_{\boldsymbol{\theta}} \mathcal{L}(\cdot; \mathbf{x})\| = \mathcal{O}(L)$, as is stipulated by the bound $\epsilon' < \sigma^2/\mu = \mathcal{O}(L)$. Now, setting $\delta \geq 2 \exp \left(-k_r \cdot \frac{\epsilon'^2}{8\sigma^2} \right)$, and using the fact that $\epsilon'^2/\sigma^2 = \mathcal{O}(1)$, and re-arranging terms, we get that if $k_r \geq \mathcal{O}(\log(1/\delta) \frac{1}{\epsilon^2})$, with probability at least $1 - \delta$, (4) is upper bounded by $\epsilon \|\nabla_{\boldsymbol{\theta}} \mathcal{L}(\cdot; \mathbf{x})\|$ as desired.

(2.2) Next, let us consider the gradient of $\mathcal{L}_{\text{ASTRA}}$ with respect to classifiers \mathbf{W} . Our goal is to bound the likelihood of the bad event that $\|\nabla_{\mathbf{W}} \mathcal{L}_{\text{ASTRA}}(\cdot; \mathbf{x}) - \nabla_{\mathbf{W}} \mathcal{L}(\cdot; \mathbf{x})\| \geq \epsilon \|\nabla_{\mathbf{W}} \mathcal{L}(\cdot; \mathbf{x})\|$, for a given $\epsilon > 0$. The gradient is a $d \times L$ matrix, where the ℓ th column has the gradient of the loss w.r.t.

\mathbf{w}_ℓ , and the $\|\cdot\|$ denotes the L_2 norm of the vectorized matrix. Here, we can not apply Bernstein inequality as in the above case. But, we can try to bound the differences directly as follows.

Denote by $\widehat{\mathbf{g}}_\ell$ the ℓ th column in the gradient matrix for $\mathcal{L}_{\text{ASTRA}}$ and by \mathbf{g}_ℓ the ℓ th column in the gradient matrix for \mathcal{L} . Note that for $\ell \in \mathcal{R}$, $\widehat{\mathbf{g}}_\ell - \mathbf{g}_\ell = 0$. And $\|\widehat{\mathbf{g}}_\ell - \mathbf{g}_\ell\| = \|\mathbf{g}_\ell\|$ for the labels that are not sampled. So, using the vectorized L_2 -norm,

$$\|\nabla_{\mathbf{W}} \mathcal{L}_{\text{ASTRA}}(\cdot; \mathbf{x}) - \nabla_{\mathbf{W}} \mathcal{L}(\cdot; \mathbf{x})\|^2 = \sum_{\ell \notin \mathcal{R}} \|\mathbf{g}_\ell\|^2.$$

We can apply Chernoff bounds to control the deviation from the true gradient, which gives

$$\begin{aligned} P\left(\|\nabla_{\mathbf{W}} \mathcal{L}_{\text{ASTRA}}(\cdot; \mathbf{x}) - \nabla_{\mathbf{W}} \mathcal{L}(\cdot; \mathbf{x})\| \geq \epsilon \|\nabla_{\mathbf{W}} \mathcal{L}(\cdot; \mathbf{x})\|\right) & \quad (5) \\ & \leq \frac{\mathbb{E}[\exp(s \cdot \|\nabla_{\mathbf{W}} \mathcal{L}_{\text{ASTRA}}(\cdot; \mathbf{x}) - \nabla_{\mathbf{W}} \mathcal{L}(\cdot; \mathbf{x})\|)]}{\exp(s \cdot \epsilon \|\nabla_{\mathbf{W}} \mathcal{L}(\cdot; \mathbf{x})\|)} & (6) \\ & = \frac{\mathbb{E}[\exp(s \cdot \sqrt{\sum_{\ell \notin \mathcal{R}} \|\mathbf{g}_\ell\|^2})]}{\exp(s \cdot \epsilon \|\nabla_{\mathbf{W}} \mathcal{L}(\cdot; \mathbf{x})\|)}. & (7) \end{aligned}$$

Now consider $\|\mathbf{g}_\ell\| = \left\| \frac{1}{1 + \exp(-\mathbf{w}_\ell^T \Phi(\mathbf{x}))} \Phi(\mathbf{x}) \right\| \leq c$, where c is a constant the depends on the bound of the embedding and classifier norms. We can bound $\mathbb{E}[\exp(s \cdot \sqrt{\sum_{\ell \notin \mathcal{R}} \|\mathbf{g}_\ell\|^2})] \leq \exp(s \cdot (L - k_r)c)$, so (7) becomes:

$$\text{RHS of (7)} \leq \exp(s \cdot (L - k_r)c) \cdot \exp(-s \cdot \epsilon \|\nabla_{\mathbf{W}} \mathcal{L}(\cdot; \mathbf{x})\|) \leq \exp(s \cdot (L - k_r)c).$$

We can choose $s > 0$ that optimizes the upper bound, i.e., probability of the bad event that $\|\nabla_{\mathbf{W}} \mathcal{L}_{\text{ASTRA}}(\cdot; \mathbf{x}) - \nabla_{\mathbf{W}} \mathcal{L}(\cdot; \mathbf{x})\| \geq \epsilon \|\nabla_{\mathbf{W}} \mathcal{L}(\cdot; \mathbf{x})\|$, above.

This concludes the proof of the Lemma.

A.2 Proof of Theorem 4.2

We will state a smoothness assumption on the loss function.

Assumption A.1. The loss \mathcal{L} is H -smooth in its parameters $\boldsymbol{\theta}$, \mathbf{W} , i.e., for all valid parameters $(\boldsymbol{\theta}_1, \mathbf{W}_1)$, $(\boldsymbol{\theta}_2, \mathbf{W}_2)$, we have:

$$\mathcal{L}(\boldsymbol{\theta}_1, \mathbf{W}_1) \leq \mathcal{L}(\boldsymbol{\theta}_2, \mathbf{W}_2) + \langle \nabla \mathcal{L}(\boldsymbol{\theta}_2, \mathbf{W}_2), [\boldsymbol{\theta}_1 - \boldsymbol{\theta}_2; \mathbf{W}_1 - \mathbf{W}_2] \rangle + \frac{H}{2} \|[\boldsymbol{\theta}_1 - \boldsymbol{\theta}_2; \mathbf{W}_1 - \mathbf{W}_2]\|_2^2.$$

Lemma 4.1 suggests that during every epoch, Algorithm 1 has access to a biased gradient oracle, i.e., for some $\epsilon \in (0, 1)$, for all epochs t , with high probability, we have the vectorized-gradient of the loss with respect to the parameters $\boldsymbol{\theta}$ and \mathbf{W} at epoch t , say $\mathbf{g}^{(t)}$, can be written as $\mathbf{g}^{(t)} = \nabla \mathcal{L}(\boldsymbol{\theta}^{(t)}, \mathbf{W}^{(t)}) + \Delta^{(t)}$, where $\|\Delta^{(t)}\|_2 \leq \epsilon \cdot \|\nabla \mathcal{L}(\boldsymbol{\theta}^{(t)}, \mathbf{W}^{(t)})\|_2$. If we choose the learning rate η as stated in the Theorem, then we satisfy the pre-requisites of Lemma 7 in the Appendix of [8]. The convergence guarantee as given in the statement of the Theorem follows, with constants as specified in Lemma 7 of [8]. This concludes the proof.

B Implementation Details

B.1 Datasets

In this subsection, we provide more details on the datasets used for our experiments. We compare ASTRA on short-text datasets such as LF-AmazonTitles-131K, LF-AmazonTitles-1.3M and long-text datasets such as LF-Amazon-131K and LF-Wikipedia-500K. All these four datasets are with label features. We also evaluate on Amazon-670K and Amazon-3M datasets which are without label

Table 9: Dataset statistics. All the public datasets can be downloaded from the XC repository [4].

Dataset	Type	# Training Points	# Labels	# Test points	Avg. # datapts. per label	Avg. # labels per datap.
Datasets without label features						
Amazon-670K	Full-text	490,449	670,091	153,025	3.9	5.5
Amazon-3M	Full-text	1,717,899	2,812,281	742,507	22.0	36.0
Datasets with label features						
LF-AmazonTitles-131K	Short-text	294,805	131,073	134,835	2.3	5.2
LF-AmazonTitles-1.3M	Short-text	2,248,619	1,305,265	970,237	22.2	38.2
LF-Amazon-131K	Full-text	294,805	131,073	134,835	2.3	5.2
LF-Wikipedia-500K	Full-text	1,813,391	501,070	783,743	4.8	24.8
Proprietary Datasets						
SS-20M	Short-text	146,193,053	19,049,952	16,629,030	199.7	26.0
SS-120M	Short-text	370,080,440	120,293,341	92,532,582	10.4	10.4

Table 10: This table contains the % of labels in each decile for LF-AmazonTitles-131K and SS-120M datasets and show that their head and tail distributions are similar

Decile	10	9	8	7	6	5	4	3	2	1
LF-AmazonTitles-131K	0.3%	1.0%	1.8%	2.8%	4.3%	6.4%	9.4%	14.0%	21.5%	38.5%
SS-120M	1.2%	3.1%	4.5%	5.9%	7.3%	8.9%	10.9%	13.5%	17.8%	26.9%

features. We also report results on proprietary datasets with 20 million and 120 million labels. These datasets cover a variety of applications including product-to-product recommendation (Amazon-670K, Amazon-3M, LF-Amazon-131K, LF-AmazonTitles-131K, and LF-AmazonTitles-1.3M), predicting Wikipedia categories (LF-Wikipedia-500K) and matching user queries to advertiser bid phrases in sponsored search (SS-20M, SS-120M) Table 9 in the Appendix gives statistic of these datasets. In addition to the aggregate statistics in Table 9, we did a decile-wise analysis of SS-120M and LF-AmazonTitles-131K to compare the characteristics of the proprietary dataset with academic dataset. We divided the labels into 10 deciles based on number of training points and calculate the number of labels in each decile to show that the proprietary dataset has similar distribution of head and tail labels. Table 10 in the Appendix has the decile-wise analysis. Similar to Renée, we augment the training data with label texts as training data-points with the corresponding label id as a positive label.

B.2 Hyperparameter Tuning

For ASTRA, we use the same values as that of Renée for hyperparameters batch-size and weight decay. We tune dropout in the range [0.5-0.9] on a small validation set and observe that higher dropout performs better across datasets. We tune learning rate for ASTRA in range [$10 * lr_Renée$, $0.1 * lr_Renée$] for both encoder and classifier on a small validation set. In general, we observe that higher lr values yield good performance. Similarly, we tune warmup in range [2000-10000] on a small validation set and observe that lower warmup values help perform better. As ASTRA achieves convergence faster than Renée, the number of epochs for ASTRA is smaller than Renée for many datasets.

There are three hyperparameters for negative sampling: k_p , k_r and k_h . k_p : For all public datasets, we simply use all the available +ve labels for the data points. e.g., $k_p = 7$, which is the max. no. of +ve labels for any data point, for LF-AmazonTitles-131K; in case a data point has fewer positives than 7, we simply pad that with random negatives.

k_r, k_h : We tune k_r in (1600,3200,4800,6400) and k_h in (160,240,320,400,480,560,640,720,800) on a small validation set and pick the one that works best. In general, we have observed that the skewed ratio $k_r:k_h$ in range(10:1 to 5:1) works better across datasets.

We tuned τ_s in (5,10,20,40) and τ_r in range (5,10,20) for 2 datasets, LF-AmazonTitles-131K and LF-AmazonTitles-1.3M. In general setting both the values to 5 seems to work the best, hence we use the same value for all other datasets.

Table 11: Hyperparameter values of ASTRA to facilitate reproducibility. The batch-size, k_p , k_h and k_r values are per GPU, when run on 16 GPUs. The ANNS index start epoch τ_s and refresh interval τ_r are both set as 5 for all the datasets.

Dataset	batch-size	epochs	lr (encoder)	lr (classifier)	dropout	warmup	weight decay (classifier)	k_r	k_h	k_p
LF-AmazonTitles-131K	32	75	0.00001	0.05	0.85	3000	0.0001	400	50	7
LF-Amazon-131K	32	100	0.0001	0.05	0.75	5000	0.0001	100	15	7
LF-Wikipedia-500K	128	40	0.0001	0.002	0.7	2500	0.001	200	30	13
LF-AmazonTitles-1.3M	64	100	0.000003	0.01	0.75	5000	0.0001	100	15	79
Amazon-670K	16	70	0.00004	0.01	0.8	10000	0.001	400	50	7
Amazon-3M	16	60	0.00004	0.01	0.75	10000	0.001	400	50	50

B.3 Break-up of iteration time

Table 3 shows the break-up of iteration time for three datasets. The different steps involved in an iteration are -

- Data Preparation: This includes creating a batch of data-points along with their positives and negatives. This is done on CPU when the training is going on GPU.
- CopyDataToGPU: This involves copying prepared data to GPU.
- EncFwdPass: This refers to the encoder forward pass where the input data-points are passed through the encoder to generate the embeddings.
- ClfFwdPass: This refers to the classifier forward pass which involves matrix multiplication $O(L)$ in *Renée*. This becomes the main bottleneck as L increases. ASTRA helps reduce this matrix multiplication to $O(\log(L))$.
- BwdPass: This refers to the backward pass of both the encoder and the classifier.

B.4 Data and Model Parallel Training

As mentioned in Section 3.2, ASTRA implements data-parallel training for encoder and model-parallel training for classifier in multi-GPU setting. Consider a scenario with G GPUs, L labels, and B batch size. In multi-GPU setting, the encoder will produce the embeddings of the input queries in parallel, with each GPU processing $\frac{B}{G}$ input queries. An all-gather call is then used to distribute the embeddings to all GPUs to attain the classifiers. The classifiers are divided across GPUs, each GPU processing $\frac{L}{G}$ classifiers. The model-parallel approach helps in speeding up the hard-negative retrieval process as well. For very large datasets, instead of building ANNS index on L labels, multiple ANNS indices are built on, one per GPU using $\frac{L}{G}$ labels present on that GPU. To further optimize memory and compute, we use a bottleneck layer that reduces the classifier dimension to 64 for large datasets similar to *Renée*.

C Additional Results

This section additional results for all the datasets which were not covered in the main paper.

Table 12: Detailed results on short-text datasets. TT refers to training time in hours on a single Nvidia V100 GPU.

Method	P@1	P@3	P@5	N@3	N@5	PSP@1	PSP@3	PSP@5	PSN@3	PSN@5	TT
LF-AmazonTitles-1.3M											
ASTRA	55.71	48.95	44.26	53.22	52.06	30.23	34.42	36.84	33.36	35.27	24.86
Renée	56.04	49.91	45.32	54.21	53.15	28.54	33.38	36.14	32.15	34.18	27.33
DEXA	55.76	48.07	42.95	52.81	51.34	30.01	33.37	35.29	32.7	34.33	103.13
DEXA (ensemble)	56.63	49.05	43.90	53.81	52.37	29.12	32.69	34.86	32.02	33.86	103.13
NGAME	54.69	47.76	42.8	52.21	50.85	28.23	32.26	34.48	31.29	33.04	97.75
NGAME (ensemble)	56.75	49.19	44.09	53.84	52.41	29.18	33.01	35.36	32.07	33.91	97.75
DEXML	58.40	-	45.46	-	54.30	-	-	36.58	-	-	~2K
SiameseXML	49.02	42.72	38.52	46.38	45.15	27.12	30.43	32.52	29.41	30.9	9.89
ECLARE	50.14	44.09	40	47.75	46.68	23.43	27.9	30.56	26.67	28.61	70.59
GalaXC	49.81	44.23	40.12	47.64	46.47	25.22	29.12	31.44	27.81	29.36	9.55
DECAF	50.67	44.49	40.35	48.05	46.85	22.07	26.54	29.3	25.06	26.85	74.47
Astec	48.82	42.62	38.44	46.11	44.8	21.47	25.41	27.86	24.08	25.66	18.54
AttentionXML	45.04	39.71	36.25	42.42	41.23	15.97	19.9	22.54	18.23	19.6	380.02
MACH	35.68	31.22	28.35	33.42	32.27	9.32	11.65	13.26	10.79	11.65	60.39
X-Transformer	-	-	-	-	-	-	-	-	-	-	-
LightXML	-	-	-	-	-	-	-	-	-	-	-
AnneXML	47.79	41.65	36.91	44.83	42.93	15.42	19.67	21.91	18.05	19.36	2.48
DiSMEC	-	-	-	-	-	-	-	-	-	-	-
Parabel	46.79	41.36	37.65	44.39	43.25	16.94	21.31	24.13	19.7	21.34	1.5
XT	40.6	35.74	32.01	38.18	36.68	13.67	17.11	19.06	15.64	16.65	82.18
Slice	34.8	30.58	27.71	32.72	31.69	13.96	17.08	19.14	15.83	16.97	0.79
PfastreXML	37.08	33.77	31.43	36.61	36.61	28.71	30.98	32.51	29.92	30.73	9.66
Bonsai	47.87	42.19	38.34	45.47	44.35	18.48	23.06	25.95	21.52	23.33	7.89
XR-Transformer	50.14	44.07	39.98	47.71	46.59	20.06	24.85	27.79	23.44	25.41	132
LF-AmazonTitles-131K											
ASTRA	46.20	30.72	21.95	47.43	49.57	39.36	47.43	50.57	43.81	46.46	2.02
Renée	46.05	30.81	22.04	47.46	49.68	39.08	45.12	50.48	43.56	46.24	2.05
DEXA	45.78	30.13	21.29	46.49	48.37	38.57	43.95	48.56	42.44	44.76	13.01
DEXA (ensemble)	46.42	30.50	21.59	47.06	49.00	39.11	44.69	49.65	43.10	45.58	13.01
NGAME	44.95	29.87	21.20	45.95	47.92	38.25	43.75	48.42	42.18	44.53	12.59
NGAME (ensemble)	46.01	30.28	21.47	46.69	48.67	38.81	44.4	49.43	42.79	45.31	12.59
DEXML	42.52	-	20.64	-	46.33	-	-	47.40	-	-	83.33
SiameseXML	41.42	27.92	21.21	42.65	44.95	35.80	40.96	46.19	39.36	41.95	1.08
ECLARE	40.74	27.54	19.88	42.01	44.16	33.51	39.55	44.7	37.7	40.21	2.16
GalaXC	39.17	26.85	19.49	40.82	43.06	32.5	38.79	43.95	36.86	39.37	0.42
DECAF	38.4	25.84	18.65	39.43	41.46	30.85	36.44	41.42	34.69	37.13	2.16
Astec	37.12	25.2	18.24	38.17	40.16	29.22	34.64	39.49	32.73	35.03	1.83
AttentionXML	32.25	21.7	15.61	32.83	34.42	23.97	28.6	32.57	26.88	28.75	20.73
MACH	33.49	22.71	16.45	34.36	36.16	24.97	30.23	34.72	28.41	30.54	3.3
X-Transformer	29.95	18.73	13.07	28.75	29.6	21.72	24.42	27.09	23.18	24.39	64.4
LightXML	35.6	24.15	17.45	36.33	38.17	25.67	31.66	36.44	29.43	31.68	71.4
BERTXML	38.89	26.17	18.72	39.93	41.79	30.1	36.81	41.85	34.8	37.28	12.55
ELIAS	40.13	27.11	19.54	-	-	31.05	37.57	42.88	-	-	-
AnneXML	30.05	21.25	16.02	31.58	34.05	19.23	26.09	32.26	23.64	26.6	0.08
DiSMEC	35.14	23.88	17.24	36.17	38.06	25.86	32.11	36.97	30.09	32.47	3.1
Parabel	32.6	21.8	15.61	32.96	34.47	23.27	28.21	32.14	26.36	28.21	0.03
XT	31.41	21.39	15.48	32.17	33.86	22.37	27.51	31.64	25.58	27.52	9.46
Slice	30.43	20.5	14.84	31.07	32.76	23.08	27.74	31.89	26.11	28.13	0.08
PfastreXML	32.56	22.25	16.05	33.62	35.26	26.81	30.61	34.24	29.02	30.67	0.26
Bonsai	34.11	23.06	16.63	34.81	36.57	24.75	30.35	34.86	28.32	30.47	0.1
XR-Transformer	38.1	25.57	18.32	38.89	40.71	28.86	34.85	39.59	32.92	35.21	35.4

Table 13: Detailed results on long-text dataset. TT refers to training time in hours on a single Nvidia V100 GPU.

Method	P@1	P@3	P@5	N@3	N@5	PSP@1	PSP@3	PSP@5	PSN@3	PSN@5	TT
LF-Amazon-131K											
ASTRA	47.13	31.29	22.35	48.23	50.47	39.14	46.07	51.93	44.32	47.28	7.92
Renée	48.05	32.33	23.26	49.56	52.04	40.11	47.39	53.67	45.37	48.52	6.97
DEXA	47.12	31.35	22.35	48.06	50.22	38.86	45.17	50.59	43.29	45.99	41.41
DEXA (ensemble)	47.16	31.45	22.42	48.2	50.36	38.7	45.43	50.97	43.44	46.19	41.41
NGAME	46.53	30.89	22.02	47.44	49.58	38.53	44.95	50.45	43.07	45.81	39.99
NGAME (ensemble)	46.65	30.95	22.03	47.51	49.61	38.67	44.85	50.12	43	45.64	39.99
SiameseXML	44.81	30.19	21.94	46.15	48.76	37.56	43.69	49.75	41.91	44.97	1.18
ECLARE	43.56	29.65	21.57	45.24	47.82	34.98	42.38	48.53	40.3	43.37	2.15
GalaXC	41.46	28.04	20.25	43.08	45.32	35.1	41.18	46.38	39.55	42.13	0.45
DECAF	42.94	28.79	21	44.25	46.84	34.52	41.14	47.33	39.35	42.48	1.8
Astec	42.22	28.62	20.85	43.57	46.06	32.95	39.42	45.3	37.45	40.35	3.05
AttentionXML	42.9	28.96	20.97	44.07	46.44	32.92	39.51	45.24	37.49	40.33	50.17
MACH	34.52	23.39	17	35.53	37.51	25.27	30.71	35.42	29.02	31.33	13.91
LightXML	41.49	28.32	20.75	42.7	45.23	30.27	37.71	44.1	35.2	38.28	56.03
BERTXML	42.59	28.39	20.27	43.57	45.61	33.55	40.83	46.4	38.8	41.61	48.11
AnneXML	35.73	25.46	19.41	37.81	41.08	23.56	31.97	39.95	29.07	33	0.68
DiSMEC	41.68	28.32	20.58	43.22	45.69	31.61	38.96	45.07	36.97	40.05	7.12
Parabel	39.57	26.64	19.26	40.48	42.61	28.99	35.36	40.69	33.36	35.97	0.1
XT	34.31	23.27	16.99	35.18	37.26	24.35	29.81	34.7	27.95	30.34	1.38
Slice	32.07	22.21	16.52	33.54	35.98	23.14	29.08	34.63	27.25	30.06	0.11
PfastreXML	35.83	24.35	17.6	36.97	38.85	28.99	33.24	37.4	31.65	33.62	1.54
Bonsai	40.23	27.29	19.87	41.46	43.84	29.6	36.52	42.39	34.43	37.34	0.4
XR-Transformer	45.61	30.85	22.32	47.1	49.65	34.93	42.83	49.24	40.67	43.91	38.4
LF-Wikipedia-500K											
ASTRA	84.88	65.87	51.30	79.45	77.44	39.26	51.04	56.11	50.05	54.98	40.36
Renée	84.95	66.25	51.68	79.79	77.83	39.89	51.77	56.70	50.73	55.57	180.00
DEXA	84.92	65.5	50.51	79.18	76.8	42.59	53.93	58.33	52.92	57.44	57.51
DEXA (ensemble)	83.52	65.02	50.85	78.4	76.69	42.15	51.89	57.38	51.36	56.46	-
NGAME	84.01	64.69	49.97	78.25	75.97	41.25	52.57	57.04	51.58	56.11	54.88
NGAME (ensemble)	84.01	64.69	49.97	78.25	75.97	41.25	52.57	57.04	51.58	56.11	54.88
DEXML	85.78	-	50.53	-	77.11	-	-	58.97	-	-	~592
SiameseXML	67.26	44.82	33.73	56.64	54.29	33.95	35.46	37.07	36.58	38.93	4.37
ECLARE	68.04	46.44	35.74	58.15	56.37	31.02	35.39	38.29	35.66	38.72	9.4
GalaXC	55.26	35.07	26.13	45.51	43.7	31.82	31.26	32.47	32.75	34.5	-
DECAF	73.96	54.17	42.43	66.31	64.81	32.13	40.13	44.59	39.57	43.7	44.23
Astec	73.02	52.02	40.53	64.1	62.32	30.69	36.48	40.38	36.33	39.84	20.35
AttentionXML	82.73	63.75	50.41	76.56	74.86	34	44.32	50.15	42.99	47.69	110.6
MACH	52.78	32.39	23.75	42.05	39.7	17.65	18.06	18.66	19.18	20.45	-
X-Transformer	76.95	58.42	46.14	-	-	-	-	-	-	-	-
LightXML	81.59	61.78	47.64	74.73	72.23	31.99	42	46.53	40.99	45.18	185.56
AnneXML	64.64	43.2	32.77	54.54	52.42	26.88	30.24	32.79	30.71	33.33	15.50
DiSMEC	70.2	50.6	39.7	42.1	40.5	31.2	33.4	37	33.7	37.1	-
Parabel	68.7	49.57	38.64	60.51	58.62	26.88	31.96	35.26	31.73	34.61	2.72
XT	64.48	45.84	35.46	-	-	-	-	-	-	-	-
PfastreXML	59.5	40.2	30.7	30.1	28.7	29.2	27.6	27.7	28.7	28.3	63.59
Bonsai	69.2	49.8	38.8	60.99	59.16	27.46	32.25	35.48	-	-	-
XR-Transformer	81.62	61.38	47.85	74.46	72.43	33.58	42.97	47.81	42.21	46.61	318.9

Table 14: Detailed results on the proprietary datasets with 20M and 120M labels comparing ASTRA with SOTA XC methods.

Methods	SS-20M (N = 146M, V = 2 GPUs)					SS-120M (N = 370M, V = 8 GPUs)				
	P@1	P@3	P@5	TT (hrs)	Speed-up	P@1	P@3	P@5	TT (hrs)	Slowdown
NGAME	70.46	52.32	43.94	295.83	2.3x	-Not-scalable-				
Renée	<u>71.32</u>	<u>54.33</u>	46.64	520.83	4x	83.78	55.30	<u>41.27</u>	375.16	15x
ASTRA	71.62	54.53	<u>46.60</u>	130.23	1x	<u>83.37</u>	<u>55.17</u>	41.67	25.04	1x

Table 15: Detailed results on ablative study of negative mining strategies in ASTRA on three datasets. In all the rows, the total number of negative labels per query is fixed (to 2K). Hard negatives obtained using label embeddings are denoted as “ \mathcal{E}_θ -hard”; hard negatives obtained using classifiers are denoted as “w-hard”. “Curriculum learning” denotes gradually increasing the ratio of w-hard : random negatives through the training epochs. *All the hard negatives are stale (refreshed every 5 epochs)*. The best results are in **bold**; the second best underlined.

Negative Sampling Strategy	LF-AmazonTitles-131K			LF-Amazon-131K			LF-Wikipedia-500K		
	P@1	P@3	P@5	P@1	P@3	P@5	P@1	P@3	P@5
random	44.57	30.24	<u>21.83</u>	45.62	31.28	22.90	72.49	55.85	44.58
\mathcal{E}_θ -hard	41.98	27.63	19.07	15.39	11.34	8.65	57.37	38.29	28.87
random + \mathcal{E}_θ -hard	45.55	30.24	21.55	45.79	30.74	22.15	81.40	61.98	47.60
curriculum Learning (\mathcal{E}_θ hard)	45.84	30.53	21.75	43.81	29.44	21.25	74.35	58.30	46.24
w-hard	41.74	28.60	20.79	17.86	11.96	8.87	52.84	33.30	22.92
Curriculum learning	<u>45.83</u>	30.40	21.58	47.33	31.50	<u>22.47</u>	84.56	66.23	51.72
random + w-hard (ASTRA)	46.20	30.51	21.95	<u>47.13</u>	<u>31.29</u>	22.35	84.88	<u>66.09</u>	<u>51.30</u>

Table 16: Results (Precision@k) on public short-text datasets without label features comparing ASTRA with state-of-the-art XC methods. Results for LightXML, Renée are from Jain et al. [21], DEXA and NGAME are from Dahiya et al. [10]; and CascadeXML and ELIAS numbers are reported from Buvanesh et al. [5]. The best results are in **bold**; the second best underlined.

Methods	Amazon-670K						Amazon-3M					
	P@1	P@3	P@5	PSP@1	PSP@3	PSP@5	P@1	P@3	P@5	PSP@1	PSP@3	PSP@5
AttentionXML	47.14	42.7	38.99	32.13	35.14	37.82	50.86	48.04	45.83	15.52	18.45	20.6
XR-Transformer	49.11	43.8	40.00	29.90	34.35	38.63	52.60	49.40	46.90	16.54	19.94	22.39
LightXML	47.30	42.20	38.50	-	-	-	-Not-scalable-					
ELIAS	48.68	43.78	40.04	31.22	34.94	38.31	49.93	47.07	44.85	14.97	17.46	19.34
CascadeXML	48.80	43.80	40.1	31.40	36.22	40.28	51.30	49.00	46.90	-	-	-
Renée	54.23	48.22	43.83	34.16	39.14	43.39	54.84	52.08	49.77	15.74	<u>19.06</u>	21.34
ASTRA	<u>53.05</u>	<u>47.28</u>	<u>42.96</u>	<u>33.21</u>	<u>38.40</u>	<u>42.78</u>	<u>52.75</u>	<u>49.73</u>	<u>47.40</u>	<u>15.78</u>	<u>18.97</u>	<u>21.37</u>

Table 17: Comparison of dualencoder models with ASTRA.

Method	LF-AmazonTitles-131K		LF-AmazonTitles-1.3M		LF-Wikipedia-500K	
	P@1	P@5	P@1	P@5	P@1	P@5
DEXML	42.52	20.64	58.40	45.46	85.78	<u>50.53</u>
DEXA	44.76	21.18	51.92	38.86	79.99	42.52
NGAME	42.61	20.69	45.82	35.48	77.92	40.95
ANCE	42.67	20.98	46.44	37.59	63.33	43.35
DPR	41.85	20.88	44.64	34.83	65.23	45.85
ASTRA	46.20	21.95	<u>55.71</u>	<u>44.26</u>	<u>84.88</u>	51.30

Table 18: Ablation study on the effect of augmenting training data with label text on ASTRA accuracy.

Methods	LF-AmazonTitles-131K		LF-Wikipedia-500K	
	P@1	P@5	P@1	P@5
ASTRA(without data augmentation)	44.81	21.64	82.88	49.20
ASTRA(with data augmentation)	46.20	21.95	84.88	51.30

Table 19: Results with 95% confidence intervals for LF-AmazonTitles-131K and LF-Wikipedia-500K

LF-AmazonTitles-131K			LF-Wikipedia-500K		
P@1	P@3	P@5	P@1	P@3	P@5
46.15 ± 0.037	30.72 ± 0.095	21.91 ± 0.094	84.88 ± 0.093	65.87 ± 0.076	51.30 ± 0.065